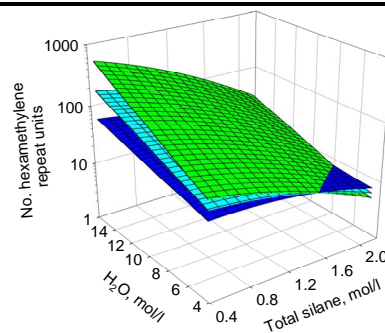Mary Ann B. Meador, Lynn A. Capadona, Linda McCorkle, Demetrios S. Papadopoulos and Nicholas Leventis

Structure-property relationships in porous 3-D nanostructures as a function of preparation conditions: isocyanate cross-linked silica aerogels

Aerogels produced by cross-linking amine decorated silica surfaces with di-isocyanates are significantly stronger than native aerogels with only a small effect on density or porosity. Herein, we examine the effects of four processing parameters on properties of resulting monoliths, focusing on ^{13}C NMR to give insight into the polymer cross-link.

For Table of Contents use only: Manuscript No. CM070102P

STRUCTURE-PROPERTY RELATIONSHIPS IN POROUS 3-D NANOSTRUCTURES AS A FUNCTION OF PREPARATION CONDITIONS: ISOCYANATE CROSS-LINKED SILICA AEROGELS

Mary Ann B. Meador,[*] *Lynn A. Capadona,*[*] *Linda McCorkle,*[†] *Demetrios S. Papadopoulos,*[‡] *and Nicholas Leventis*[§]

NASA Glenn Research Center, 21000 Brookpark Road, Cleveland, OH 44135

TITLE RUNNING HEAD: Structure-property relationships in isocyanate cross-linked aerogels

ABSTRACT. Sol-gel derived silica aerogels are attractive candidates for many unique thermal, optical, catalytic, and chemical applications because of their low density and high mesoporosity. However, their inherent fragility has restricted use of aerogel monoliths to applications where they are not subject to any load. We have previously reported cross-linking the mesoporous silica structure of aerogels with di-isocyanates, styrenes or epoxies reacting with amine decorated silica surfaces. These approaches

[*] To whom correspondence should be addressed: maryann.meador@nasa.gov, lynn.a.capadona@nasa.gov

[†] Employed through the Ohio Aerospace Institute, 22800 Cedar Point Road, Cleveland, Ohio, 44142

[‡] Employed through the University of Akron, Akron, OH 44325

[§] Current address: Department of Chemistry, University of Missouri—Rolla, Rolla, Missouri, 65409

have been shown to significantly increase the strength of aerogels with only a small effect on density or porosity. Though density is a prime predictor of properties such as strength and thermal conductivity for aerogels, it is becoming clear from previous studies that varying the silica backbone and size of the polymer cross-link independently can give rise to combinations of properties which cannot be predicted from density alone. Herein, we examine the effects of four processing parameters for producing this type of polymer cross-linked aerogel on properties of the resulting monoliths. We focus on the results of ^{13}C CP-MAS NMR which gives insight to the size and structure of polymer cross-link present in the monoliths, and relates the size of the cross-links to microstructure, mechanical properties and other characteristics of the materials obtained.

KEYWORDS: Polymer cross-linked aerogels, sol-gel, di-isocyanates, supercritical fluid extraction.

Introduction

Sol-gel derived silica aerogels are attractive candidates for many unique thermal, optical, catalytic, and chemical applications[1] because of their low density and high mesoporosity. However, their inherent fragility has restricted the use of aerogel monolithic materials to, for example, insulation in extreme temperature environments such as in the insulated boxes containing the batteries and electronics for the Mars Rovers.[2] Various strategies to improve the physical properties of monolithic aerogels have been investigated over the past ten years. For example, Novak et al[3] reported some improvement in aerogel compressive strength by introducing linear polyvinylpyridine into the silica network, and cross-linking the polymer through the addition of $CuCl_2$. Thus, it was suggested that the loads were distributed between two interpenetrating, three-dimensional cross-linked networks instead of one. Others have incorporated organic linking groups, like polydimethylsiloxane[4] or a polybenzobisthiazole[5] into the silica structure by co-reacting the oligomers with the alkoxysilanes in the sol-gel process, greatly reducing brittleness and increasing deformability in the aerogel.

Previously, we have reported cross-linking the mesoporous silica structure of an aerogel by reacting di-isocyanates with silanols on the surface of wet gels before supercritical drying.[6,7] We have also examined cross-linking amine-decorated silica frameworks with epoxies as the cross-link.[8] The nanocast polymers form a conformal coating over the surface of the 3-D silica framework, serving to reinforce this framework by widening the neck regions between neighboring nanoparticles. Either approach has been shown to significantly increase the strength of the aerogel as much as two orders of magnitude while only doubling the density. Aerogels with densities ranging from 0.2-0.5 g/cm^3 have been made in this way, and have been shown to have very high specific strength compared to non-cross-linked native aerogels with a similar silica framework. Thus, these hybrid materials may be enabling for future space exploration missions as well as advanced aeropropulsion systems which demand lighter-weight, robust, dual purpose materials for insulation, radiation protection and/or structural elements of habitats, rovers, astronaut suits and cryotanks.

More recently, we have reported cross-linking amine decorated silica particles with di-isocyanate as shown in Scheme 1, in a process analogous to the epoxy cross-linked aerogels.[9] Compressive strength, Young's modulus and thermal conductivity were thoroughly examined for 3-aminopropyl triethoxysilane (APTES) modified di-isocyanate cross-linked aerogels with average densities of approximately 0.48g/cm^3. Ultimate compressive stress at ultimate failure for these unoptimized formulations of di-isocyanate cross-linked aerogels was found to be 186 MPa with a strain of 77%.

We have also produced much lower density di-isocyanate cross-linked aerogels by systematically reducing the mass of the underlying silica framework[10] by starting with lower concentrations of the co-polymerized silanes, tetramethylorthosilicate (TMOS) and APTES, in the starting gel. The resulting cross-linked monoliths had densities ranging from as low as 0.036 g/cm^3 up to 0.45 g/cm^3. The concentration of di-isocyanate the gels were exposed to and the reaction temperatures were also varied. While the lowest density monoliths reported in that study may not be suitable as structural solids, they are as much as 45 times stronger than uncross-linked monoliths with a similar silica framework at only

double the density. Furthermore, samples below 0.060 g/cm^3 exhibit some flexibility, indicating that at those densities the properties of the polymer begin to emerge.

Though density is a prime predictor of properties such as strength and thermal conductivity for aerogels, it is becoming clear from these previous studies that varying the silica backbone and size of the polymer cross-link independently can give rise to combinations of properties which cannot be predicted from density alone. For use as a multifunctional insulation/structural material, it is desirable to optimize the strength while reducing density and thermal conductivity as much as possible. Herein, we examine the effects of four processing parameters for producing this type of polymer cross-linked aerogel on properties of the resulting monoliths. As previously shown, the concentration of total silane (total APTES plus TMOS in a 1: 3 v/v ratio) determines, in large part, the density of the underlying silica and the concentration of di-isocyanate cross-linker used for soaking the silica gels determines both the amount and length of polymer forming the cross-links. Hence, in this study, we varied the total silane concentration from 0.44 mol/l to 2.1 mol/l in acetonitrile (CH$_3$CN), and di-isocyanate concentration from 7 to 34% by weight in CH$_3$CN. We also expanded on previous studies by varying the amount of water (3.72 to 15.27 mol/l) used to catalyze gel formation, which should have an effect on both initial gelation and chain extension/polymerization. It is also desirable to shorten the process for making the aerogels, and thereby minimize the number of wash steps necessary without compromising final properties. To this end, we have also varied the number of wash steps after gelation and before polymerization from zero to four.

A statistical experimental design methodology was employed to reduce the number of experiments and to allow computation of empirical models describing the relationship between the four variables and the measured responses. In all, 25 different runs using different combinations of the four variables plus 4 repeats were utilized to produce a total of 29 separate cross-linked aerogels. These were prepared according to Scheme 1 in random run order as listed in Table 1, and evaluated by microscopy, surface analysis, mechanical testing and measurements of skeletal and bulk density. We also focus on

the results of ^{13}C CP-MAS NMR, giving insight to the size of polymer cross-link present in the monoliths and relate this to the other properties. Finally, to assess the validity of the empirical models and test their ability to accurately predict aerogel properties, seven additional runs were produced corresponding to predicted optima. The properties of monoliths from these runs are measured and compared to the predicted values, and utilized to further refine the predictive models.

Experimental

Materials. Tetramethylorthosilicate (TMOS), 3-aminopropyltriethoxy-silane (APTES) and anhydrous acetonitrile (CH_3CN) were purchased from the Aldrich Chemical Co. Di-isocyanate oligomer (Desmodur N3200 a 1,6-hexamethylene di-isocyanate-based oligomer) was donated by Bayer Corporation. All reagents were used without further purification.

Instrumentation. Solid ^{13}C and ^{29}Si NMR spectra of the polymer cross-linked aerogels were obtained on a Bruker Avance-300 spectrometer with a 4 mm solids probe using cross polarization and magic angle spinning at 11 kHz. Carbon spectra were externally referenced to the carbonyl of glycine which appears at 176.1 relative to tetramethylsilane (TMS). Silicon spectra were externally referenced to the silicon peak of the sodium salt of 3-trimethoxysilylpropionic acid at 0 ppm. Water-content was quantified using a Mitsubishi Model CA-100, coulometric Karl-Fisher moisture analyzer. Nitrogen adsorption porosimetry was conducted on an ASAP 2000 Surface Area/Pore Size Distribution Analyzer (Micromeritics Instrument Corp). Skeletal density was measured using an Accupyc 1330 Helium Pycnometer (Micromeritics Instrument Corp). For all of these measurements, samples were outgassed at 80°C for 24 hours under vacuum. Samples for microscopy were coated with gold and viewed using a Hitachi S-4700 field-emission SEM. Thermal conductivity samples were evaluated using a NanoFlash Laser Flash Analyzer (Netzsch Instruments, LFA 447). Supercritical fluid extraction was performed with CO_2 in a 1 L Speed-SFE chamber (Applied Separations).

Preparation of di-isocyanate cross-linked aerogels. Utilizing a statistical experimental design approach, the concentration of the co-polymerized silanes and water in the starting gel, the number of

washes post-gelation and the concentration of the di-isocyanate in the cross-linking baths to which the gels are exposed were varied according to Table 1.

Amine modified silica gels were produced as previously reported[8] by combining two separate solutions, designated as A and B, in a sol-gel process. In a typical procedure using the values given in run 1 in Table 1 as an example, 2.9 ml of TMOS and 1 ml of APTES were combined together with 46.1 mL CH_3CN for solution A (0.48 mol/l total silane). The use of amine–rich APTES eliminates the need for additional base catalysis. Solution B was prepared with an equal amount of solvent and 3.9 ml water (4.30 mol/l). The solutions were independently cooled in a dry-ice/acetone bath to control premature gelation when combined. Five Norm-ject 20ml polypropylene syringes—nominally 20 mm diameter were prepared to use as molds by cutting off the needle end, extending the plunger nearly all the way out and standing them in empty jars, plunger down for support. The contents of solution B were then poured into the container with solution A which was capped immediately, shaken vigorously, then poured into the molds, and allowed to gel and age for a total of 24 hours. The wet gels were extracted into clean solvent at least five times the volume by inverting the syringes and depressing the plunger. The gels rested in the solvent for 24 hours and then the solvent was exchanged an additional three times at 24 hour intervals to remove excess water and condensation byproducts (methanol and ethanol). To cross-link with isocyanate, the solvent in each of the 5 wet gel containers was replaced with a 34% w/w (160g isocyanate in 400mL solvent) di-isocyanate bath for 24 hours with intermittent agitation. Afterwards, the monomer solution was decanted, replaced with fresh acetonitrile, and the monoliths were allowed to react for 72 hours in a 71°C oven. The oven-cured gels were then cooled to room temperature, and the solvent was replaced four more times in 24 hour intervals as before to remove any un-reacted monomer or oligomers from the mesopores of the wet gels. These gels were then placed in a 1 liter supercritical fluid extraction chamber where the solvent was exchanged with liquid CO_2 at ~100 bar and 25 $^{\circ}$C in five two hour cycles. Heating the chamber to 45 $^{\circ}$C causes the pressure to increase to ~215 bar converting the CO_2 to a supercritical state. Slow, controlled venting of

the chamber gives the resulting polymer cross-linked aerogel monoliths from run 1 with bulk densities of 0.071 g/cm^3.

Compression testing. A cylindrical specimen from each run was sectioned in half with a scroll saw to eliminate buckling in some of the more fragile specimens. Each half was nominally 18 mm in diameter and about 25.4 mm in length with a slenderness ratio of about 5.7:1.[11] The top and bottom of each specimen was sanded and checked using an L-square to make certain that these surfaces were smooth and parallel. The samples were tested between a pair of compression platens on a Model 4505 Instron load frame using the Series IX data acquisition software. The platen surfaces were coated with a graphite lubricant to reduce the surface friction and barreling of the specimen. The specimens were tested in accordance with ASTM D695 with the exception of sample size. Although the ASTM standard calls for a slenderness ratio of 11 to 16:1, typified by a cylinder 12.7 mm in diameter by 50.8 mm in length, using this sample size would have caused some of the lower density (more foamlike) specimens to buckle.

Statistical Analysis. Experimental design and analysis was conducted using the RS/Series for Windows, including RS/1 Version 6.01, and RS/Discover and RS/Explore Release 4.1, available from Domain Manufacturing Corporation, Burlington, MA.

Results and Discussion

Four preparation conditions were varied using a statistical experimental design approach, including total silane concentration (s), di-isocyanate concentration (d), water concentration (h) and the number of washes after gelation (w) as listed in Table 1. To evaluate measured properties of the di-isocyanate cross-linked aerogels as a function of these processing parameters, it was deemed reasonable to assume that linear and non-linear effects of the variables could be captured by a full-quadratic model of the form shown in Equation 1:

$$\text{Property} = A + Bs + Cd + Dh + Ew + Fs^2 + Gd^2 + Hh^2 + Iw^2 + Jsd + Ksh + Lsw + Mdh + Ndw + Ohw \qquad (1)$$

where A through O are coefficients that are empirically derived from experimental data. The model contains terms for first and second order effects of all four variables and all possible two way interactions. To evaluate first and second order effects, a minimum of three levels of each variable must be evaluated experimentally, requiring a minimum of 81 separate runs (3^4 experiments representing three levels of each of the four variables) in a full-factorial design not including repeats. To minimize the number of experiments, a d-optimal design strategy was employed in which a reduced set of experimental runs is computer-generated from the 81 candidates. In total, only 29 experiments were needed to evaluate the above model, including four repeats to assess model reliability and accuracy. The data collected from all performed tests on each of the 29 experiments is summarized in Table 1.

The initial silane concentration (total APTES plus TMOS in a 1 to 3 v/v ratio), which was varied from 0.44 to 2.10 mol/l of total silane in solution A, determines the density of underlying silica aerogel, while the amount of di-isocyanate in the cross-linking solution ranging from 6.89 to 33.9 w/w % will have the strongest effect on the degree of cross-linking as has been shown in a previous study.[10] The amount of water used in the initial gelation reaction, ranging from 3.72 to 15.27 mol/l in solution B, can affect both the underlying silica framework and polymer chain extension. Too little water, for example, might lead to incomplete hydrolysis of the alkoxysilanes.[12] In addition, as shown in Scheme 1, the isocyanate moieties can react with excess water to form amines which subsequently would react with additional isocyanate to give longer polyurea crosslinks. In the same way, the number of washes in clean solvent before polymerization (0, 2 or 4) will also affect chain extension because this affects the amount of water left in the gels. In prior studies, water was held constant at 25 v/v % of solution B (13.88 mol/l) and four washes were always used.

Empirical response surface models were derived from linear least squares regression of the experimental data so that significant effects of the variables on the measured properties could be discerned. All continuous, independent variables were orthogonalized (transformed to -1 to 1 range)

prior to modeling to minimize correlation among terms. Terms not statistically significant (<90% confidence) were dropped from the model one at a time by the stepwise modeling technique.[13] Summary statistics and significant terms in the models are shown in Table 2.

Water content. To quantify the amount of water removed from the uncross-linked gels during each washing step, aliquots were taken from used wash solvents from all four washes of a subset of the experimental runs. These aliquots were analyzed for water content by Karl Fisher titration. The data listed in Table 3 were analyzed by linear least squares regression as described above except that all terms containing di-isocyanate concentration, d, are not a factor. Selected response surface models for this data are shown in Figure 1. As evidenced from these graphs, the most water is removed in the first washing cycle while wash steps three and four remove very little additional water. The most important factor for the amount of residual water in the washes is the amount of water, h, in the initial sol. Amount of silane concentration, s, in the initial sol is also a significant factor, along with interactive effects of s*w and h*w. It is also evident from the graph that starting with the lowest amount of water, especially when starting with largest amount of silane, each washing step removes very little water, suggesting that reducing the number of washings in these gels without affecting the properties of the final monoliths may be possible.

Density. Selected response surface models for bulk density of the aerogels produced in this study are shown in Figure 2. Graphs of the densities of the corresponding cross-linked aerogels made by soaking in di-isocyanate solution after zero (green), two (cyan) and four (blue) washes are shown in Figure 2b (with the lowest polymer concentration) and 2c (with the highest polymer concentration). For both cross-linked and non-cross-linked aerogels, as expected, density significantly increases with increasing silane, water and polymer concentration, with silane concentration having the most predominant effect. Also, density decreases with increasing number of washes, especially at high concentrations of silane. This is presumably due to decreased water content in the gels available to induce chain extension reactions in the polymerization step. However, it is possible that washing also can rinse away small

silica species un-captured in the gel due to incomplete hydrolysis reaction (e.g., under low water conditions).

To get a general sense for how much density is due to polymer up-take, Figure 2a shows a graph of the densities of non-cross-linked aerogels with the same starting silane and water concentrations after four washes.[14] Comparing this graph with those in 2b and 2c, it is clear that one can obtain aerogel monoliths at similar densities which have very different relative amounts of polymer and silane. For example, a monolith with a density of 0.2 g/cm^3 that is obtained starting with the highest amount of silane and water concentration and four washes contains much less polymer (more silane) than the same density monolith prepared with lower silane concentration, and no washes.

NMR analysis. A representative selection of CP-MAS ^{13}C NMR spectra of the aerogel monoliths are shown in Figure 3. All spectra display carbonyl peaks at 157 and 159 ppm for the carbamate and polyurea structures. In addition, one of the methylenes of APTES which is bonded to Si appears at 9 ppm (peak A). The other two APTES carbons are hidden under peaks due to hexamethylene units of N3200. The two methylenes that are bonded directly to nitrogen in each of the hexamethylene repeat units of N3200 appear at 41 ppm while the four other methylenes appear at 27 ppm (peak B). Other minor peaks present in samples where water is at the lowest concentration and silane is high (for example, spectra of runs 27, 15 and 16 in Figure 3) can be attributed to ethoxy (18 ppm and 58 ppm) and methoxy (51 ppm) groups attached to Si due to incomplete hydrolysis of APTES and TMOS, respectively. This is especially evident with monoliths prepared with no washes before the polymerization step (as in Run 27), illustrating that washing before polymerization does not only remove water and alcohol by-products of condensation, but also small silica species which are present due to incomplete hydrolysis. Clearly, in unwashed samples, these get incorporated into the cross-linked structure through reaction with the di-isocyanate. Corresponding solid ^{29}Si NMR spectra for these monoliths also contain the analogous peaks due to silicon bonded to methoxy or ethoxy groups. It should be noted that the molar ratio of water to silane (R-ratio) in these runs is 1.8:1. Because water is

also a by-product of condensation, this R-ratio should theoretically be sufficient for complete hydrolysis of the APTES and TMOS mixture though in practice usually an excess of water is needed.[15]   R-ratios in this study varied from 1.8:1 up to 35:1 for those runs where silane concentration is at the lowest value and water is high (as in runs 29 and 23 also shown in Figure 3).

Peaks A and B integrated one against the other in all spectra can be used to calculate the number of repeat units of hexa-methylene di-isocyanate (HDI) between APTES terminal groups, assuming one APTES at each end. The number of HDI repeat units per cross-link analyzed in this way ranged from 3 to almost 600. Empirical models were derived relating the number of repeat units from this end-group analysis to the four variables studied. Graphs of the resulting models are shown in Figure 4 with di-isocyanate concentration held constant at 6.89% (4a) and at 33.9% (4b).

From these graphs, it can be clearly seen that all four variables have a significant effect on the length of polymer cross-link present in the final aerogel monoliths.   Comparing Figure 4a and 4b, it is evident that using higher concentrations of di-isocyanate solutions produces longer polymer chains in all cases. Increasing water concentration also increases the chain length, especially when washings are reduced or eliminated. The excess water present in such cases hydrolyzes the isocyanate groups, creating amines which are available to react with more isocyanates (see Scheme 1) forming long chains of polyurea. The largest number of repeat units (~600) per APTES is obtained where total silane is at a low, water and di-isocyanate are high and the samples are not washed before soaking in polymer. Increasing silane concentration may effectively reduce the length of cross-links, because more surface APTES amine is available for reaction with the same concentration of di-isocyanates. Thus, there may be more, but shorter, cross-links.

The number of repeat units is also decreased with increased washes before polymerization, although there is less of an effect on the number of washes when silane concentration is high and water concentration is at a low, presumably because there is not a lot of excess water present. Hence, it may be possible to eliminate washing steps by striking a balance between silane concentration and water in

the initial sol. This would considerably shorten processing time to produce the polymer cross-linked aerogels, as in the present process, each washing step adds 24 hours. However, starting with too little water as previously mentioned does detrimentally affect complete gelation, possibly producing weaker gels and consequently weaker monoliths.

Physical Properties of the cross-linked aerogels. A comparison of scanning electron micrographs (SEM) of selected samples shown in Figure 5 also gives insight into the cross-linking process. Figures 5a and 5b show micrographs of monoliths produced at low concentrations of silane, water and di-isocyanate. The sample in Figure 5a was produced with no washes (run 19) while 5b was washed four times before polymerization (run 4). There is very little difference between the two micrographs, both clearly illustrating the pearl necklace structure of an aerogel coated with polymer and the presence of much mesoporosity (dark areas). Indeed, measured properties for both samples are all very similar.

In comparison, for the monoliths shown in 5c with 0 washes (run 20) and 5d with 4 washes (run 7), water is at the highest concentration but silane and di-isocyanate concentration are low. In these micrographs, the secondary particles are larger than those in 5a and 5b. Since the samples are made starting with the same amount of silane, the larger particle size is due to an increase in the amount of polymer crosslink. Moreover, this increase in amount of polymer is more striking when the samples are made without washing before polymerization. Whereas the density of the monolith pictured in 5d is only double that of 5b, the sample made with no washes before polymerization shown in 5c is four times as dense as 5a, and the average number of HDI repeat units in the cross-links for this monolith is 9 times the size of that shown in 5a.

Increasing di-isocyanate concentration while keeping the other conditions the same as 5c (silane at a low concentration and water at high concentration), gives a monolith that appears to be nearly completely full of polymer as shown in 5e (run 23) produced from 0 washes. Indeed, run 23 was measured to have the highest number of repeat units (596) per cross-link and polymer also grew out from the surface making it impossible to accurately measure the bulk density. In contrast, the monolith

12

shown in 5f (run 2), which is made under all the same conditions as 5e except that it is washed 4 times before polymerization, looks very similar to that shown in 5d (low polymer) and measured properties are also very similar. Hence, washing four times reduces the magnitude of the effect of increasing water and increasing polymer concentration on the properties of the monoliths compared to the samples polymerized without washes.

Micrographs of monoliths produced with high concentrations of silane and di-isocyanate but low water are shown in Figure 5g from 0 washes (run 27) and 5h from 4 washes (run 16). These are similar in appearance though the monolith produced with four washes before soaking in di-isocyanate (5h) appears to have larger particles than the sample produced with 0 washes (5g). Indeed, the monolith from run 27 (shown in 5g) has an average of only 3.72 repeat units per cross-link, though the density is the highest measured in the study, while that produced in run 16 (5h) has an average of 13 repeat units per cross-link but half the measured bulk density. This must be because both runs 27 and 16, are made using water to silane mole ratio of 1.8 to 1, and thus the silanes in both runs are not completely hydrolyzed. However, as previously suggested, monoliths from run 27 should retain these less than fully reacted species through cross-linking with the polymer, while those from run 16 should actually contain less silica because the four washes will remove incomplete reaction products before cross-linking.

Monoliths shown in figures 5i and 5j were both produced with high concentrations of silane, water and di-isocyanate, but 5i was produced with no washes (run 29) and j with the maximum number of washes (run 10). The monolith pictured in 5j, still shows a large amount of porosity and an average of 14 repeat units in the cross-link, whereas that shown in 5i has very little porosity and 40 repeat units per cross-link, having most of the void space filled with polymer similar to that shown in 5e.

Percent porosity for each of the samples can be calculated from the measured bulk density ρ_b and measured skeletal density ρ_s using Equation 3. Empirical models for percent porosity shown in Figure

$$\text{Porosity \%} = (1/\rho_b - 1/\rho_s)/(1/\rho_b) \times 100 \qquad (3)$$

6 reflect some of the same observations that can be made from the micrographs in Figure 5. Samples washed four times (blue surface) maintain a high level of porosity for nearly all combinations of the other three variables, from a high of 96.6 % when di-isocyanate, water and silane concentration are all low, dipping to 75% when di-isocyanate, water and silane concentration are all high. In contrast, samples made with no washes before polymerization, ranged from immeasurably low porosity (below 50%) when di-isocyanate, water and silane concentration are all high, up to 95% when di-isocyanate, water and silane concentration are all low. Also evident from Figure 6a, the number of washes has little effect on porosity if water and polymer are held constant at the lowest value.

Mean pore diameters and surface areas were derived from nitrogen adsorption data for all the samples using the Brunauer-Emmet-Teller (BET) method. Selected response surface models for surface area are shown in Figure 7a with no cross-linking, 7b cross-linked with low di-isocyanate concentration and 7c with high di-isocyanate concentration. As can be seen from the graphs, surface area drops from a range of 400 to 700 m^2/g for the uncross-linked monoliths to a range of 8 to 320 m^2/g for those that are cross-linked. The variable with the strongest effect on surface area is the number of washes before cross-linking. Indeed, the lowest values are for those made from a combination of high water concentration and low silane, and cross-linked after no washes. Surface areas of monoliths cross-linked after washing at least twice ranged from 150 to 320 m^2/g. However, as can also be seen from Figure 7b, it is possible to make monoliths having high surface areas with no washes before cross-linking by keeping both water and di-isocyanate concentration low.

Curiously, the general relationship between water concentration and surface area changes between cross-linked and uncross-linked monoliths. Surface areas for uncross-linked monoliths decrease with decreasing water concentration (Figure 7a), while those for cross-linked monoliths show the opposite trend. The only exception is for those cross-linked with low concentration of di-isocyanate after four washes. In these instances, residual water left in the gels would be quite low. Note that under these

same conditions, the empirical model for the number of HDI repeat units (Figure 4a, blue surface) is relatively flat. The number of repeat units for monoliths produced under these conditions ranges only from 9 to 15, whereas the other plots show a much larger response to increasing water and silane concentration. It is not surprising then that the relatively uniform coating of polymer starting with low di-isocyanate across the entire range of silane and water concentration would give the same trend in surface area as the underlying silica structure. In contrast, for the other conditions, polymer build up greatly increases with increasing water and hence the opposite trend of decreasing surface area with increasing water is displayed.

Mean pore diameter from BET analysis ranging from 14 to 29 nm for uncross-linked monoliths nearly overlaps that for the cross-linked samples (10 to 26 nm). As evidenced from graphs of response surface models shown in Figure 8, total silane concentration has the largest effect on the size of the pores especially when di-isocyanate concentration is at a low, followed by a second order effect of water concentration. For uncross-linked monoliths, pore diameter is highest when silane and water concentration are low, whereas for the cross-linked monoliths, pore diameters are higher at both low and high water concentrations. High water concentration increases the number of repeat units, resulting in larger pore diameters presumably by blocking access to the smallest sized pores. Low water concentrations result in smaller number of repeat units but the average pore diameter of the underlying silica is larger.

Mechanical properties. To understand how the aerogel composition and microstructure relate to bulk mechanical behavior, compression testing was performed on all 29 samples. Typical stress-strain curves of a selection of samples are shown in Figure 9. In general, higher density samples (typified by the curve on the right showing compression of a monolith from run 8) experienced fracture ranging from ruptured cylinder walls, longitudinal cracking around the circumference, and explosive failure of the cylinder walls leaving a tire rim- shaped structure, while samples with densities below ~0.150 g/cm^3 (for example, a monolith from run 19 shown in the curve on the left) tended to flatten out or pancake

15

completely without a true breakpoint. This may be because of the arrangement of secondary particles typically seen in lower density samples. Micrographs of the aerogel samples presented in Figures 5a and 5b which are lower than $0.100g/cm^3$ show a more elongated, strand-like arrangement of the secondary particles versus the more bead-like arrangement with larger numbers of attachment points of the higher density samples. Note also that the porosities of the samples which pancaked during compression tests were all above 90%.[16]

For those samples with a defined yield in the stress-strain curves, maximum stress at the breakpoint is reported in Table 1. Strain at break was typically between 85-95% for these runs. Graphs of the empirical model for maximum stress at break are shown in Figure 10 for silane concentration ranging from 1.16 mol/L to 2.1 mol/l and di-isocyanate held constant at the lowest concentration (Figure 10a) and highest concentration (Figure 10b). Plots are also shown with water held constant at the lowest concentration (Figure 10c) and highest concentration (Figure 10d). Interestingly, as can be seen from the plots, maximum stress at break is not maximized when silane is at the highest concentration, i.e. where density is at a maximum. Rather, maximum stress at break peaks at approximately 1.5 mol/l for all levels of water and di-isocyanate concentration, as well as number of washes. One possibility is that as the total amount of silane increases, so does the amount of APTES. With more reactive sites available and the same amount of di-isocyanate, some oligomers may attach to only one APTES (dangling tethers) and not serve as a cross-link but merely as parasitic weight. It may also be that as the total amount of silane is increased, and the particle sizes and connection points between the particles increase, not all of the APTES is available at the surface for cross-linking. The graphs of the model for the number of repeat units of polymer obtained from end group analysis (Figure 4) does show a decrease with increasing total silane concentration which we interpreted *vide infra* as smaller but more cross-links. However, it could also be that larger cross-links are obtained, but are averaged over the total number of APTES groups, some of which have not participated in the cross-linking. We cannot distinguish between reacted and unreacted APTES units by ^{13}C NMR.

Ultimately, the maximum stress at break is predicted to be highest (340 MPa) when silane concentration is 1.52 mol/l, water and polymer concentration are at their highest value and the sample is washed four times before polymerization. Lengths of the polymer cross-links under these conditions are about 25 HDI repeat units. Since density is, in general, lower and porosity is relatively high when using four washes, this is also the region of the design where strength is improved while maintaining other positive properties of the aerogels. In other words, the most improvement in strength is obtained with the least penalty in density and porosity with four washes. However, as seen from Figure 10c, washing does not have as much of an effect on the maximum stress for low initial water concentration with silane concentrations below 1.3 mol/l. Under these conditions, as previously shown, the effect of the number of washings before cross-linking on either density or size of crosslink is also minimal. Consequently, cross-linked aerogel monoliths with maximum stress at break in excess of 100 MPa should be achievable with no washes before polymerization by choosing the correct di-isocyanate, water and silane concentrations. In the same way, cross-linked aerogel monoliths with a maximum stress at break approaching 200 MPa should be achievable by washing only twice before polymerization (noting the cyan colored surfaces in Figure 10a, b or d).

Off-set yield strength at 0.2% strain and Young's modulus were also extracted from each stress-strain curve, and reported in Table 1. In contrast to the maximum stress, both the graphs of offset yield shown in Figure 11 and the Young's modulus graphs shown in Figure 12 closely echo the response surface model for density presented in Figure 2. In fact, the yield stress and modulus are predicted to be at a maximum for monoliths produced with no washings at the highest concentrations of di-isocyanate, water and silane, conditions that produce samples with almost no porosity and the highest density. On the other hand, maximum stress is predicted to be highest when both modulus and offset yield are predicted to be relatively low (55 MPa and 1.5 MPa, respectively). However, it should be possible to produce cross-linked aerogel monoliths with all three properties at an acceptable level. For example, if total silane concentration is 1.5 mol/l, water concentration is 15 mol/l, and the sample is washed three

times before polymerizing with 33 w/w % di-isocyanate, the monolith produced is predicted to have a maximum stress at break of 226 MPa with an offset yield of 3.1 MPa, a modulus of 229 MPa and density of 0.35 mg/cm^3 (although porosity is predicted to be only 72 %).

Discussion of optimum runs. As already discussed, the empirical models can be used to predict properties of monoliths prepared using other combinations of di-isocyanate, water and silane than previously explored. As mentioned in the introduction, we recently reported compression properties of an unoptimized aerogel formulation cross-linked with the same di-isocyanate.[8] These monoliths averaged 0.48 g/cm^3 in density with a maximum stress at break in compression tests of 186 MPa and modulus of 120 MPa. As noted in the previous section, higher strength and modulus cross-linked monoliths with lower densities should be achievable by simply choosing the appropriate combination of the processing parameters studied.

To demonstrate the predictive capabilities of the models, a series of optimum runs in a range of densities have been formulated, synthesized and characterized as summarized in Table 4. Using the models, two different recipes were generated to produce, for example, monoliths with the highest compressive strength obtainable while keeping the densities constrained to below 0.2g/cm^3. Run 35 was predicted to maximize stress at break by using concentrations of silane, water and polymer in the mid-range of those tested with two washings before polymerization. Restricting washings to zero predicted a similar maximum stress at break, using slightly lower concentrations of water, polymer and silane (run 30). Note that washing before polymerization allows higher amounts of silane, polymer and water to be used and the compressive strength is improved by about 40% (run 35 *vs*. run 30). Runs 31, 32 and 36 were a result of optimizing the compressive strength while constraining the density to under 0.1/cm^3 and holding the number of washes to one, zero and no constraints, respectively. Finally, run 34 was the result of optimizing maximum stress while constraining the density to below 0.3 g/cm^3. The monoliths from this combination of processing conditions (run 34) have a maximum stress at break almost 30% higher then previous reported[9] with 36% lower density!

To demonstrate how well the models predict the actual data, the model-predicted (red bars) and measured values (black bars) for the data from selected responses for runs 30 through 36 are compared in Figure 13. Initial predictions were all within experimental error for the measured responses from all the additional runs. However, as more data is generated and added to the models, they become stronger and consequently are more accurate in predictive capabilities. The refined predictions (green bars) over-all show improved agreement with the measured data. Note also that all response surface models presented herein, as well as the statistical data provided in Table 2, are for the refined models using all 36 runs.

Thermal conductivity. Since aerogel utility is largely measured by insulative capability[17], we examined the thermal performance of our optimized samples at room temperature. The thermal diffusivity (α) was measured directly using a laser flash instrument (Netszch LFA 447) following ATSM E1461 and the data was fitted according the Cowan model.[18,19,20] Due to the transparency of the aerogels, a thin layer of gold was deposited on both sides of the samples, effectively eliminating radiative pathways to conduction. Following this, both sides were sprayed with dry graphite to ensure complete absorption of the laser pulse during the measurement. Using the diffusivity in combination with the measured heat capacity (C_p) of the materials obtained from differential scanning calorimetry and their bulk densities, thermal conductivity (k) can be calculated by Equation 3.

$$k = C_p \cdot \alpha \cdot \rho_b \qquad (3)$$

It is important to note that the Cowan method only accounts for heat transfer due to conduction. To obtain results encompassing both the radiation and conduction components of heat transfer directly, a steady state measurement is needed and was not used in this case due to sample size limitations. However, steady state methods have been reported for aerogel powders and monoliths that have been opacified in order to better the thermal performance by blocking the infrared component of radiant heat transfer.[21,22]

It was originally intended to measure thermal conductivity of all of the monoliths from the study and thereby to build predictive models for those data as well. However, cutting the samples into thin wafers needed for the test resulted in highly porous surfaces impossible to deposit a thin, smooth coating of gold. When the optimum runs were made, disks of the proper thickness (~1mm) for the laser flash test were made along with the cylinders. Since the molded surfaces are much less porous and tend to be resin-rich, gold could be applied in a smooth, thin layer in all but the sample from run 33, whose low density prevented proper application. Hence, thermal conductivity was measured for only the optimum runs 30-32 and 34-36 as shown in Table 3. These six data points can be considered as a screening study, allowing us to consider a model containing linear and two-way interactive terms. Multiple linear regression analysis gives the model summarized in Table 2. Total silane concentration using these few experiments over the limited range of 0.82 to 1.52 mol/l was not found to have a significant effect on thermal conductivity over and above random error. It is fully expected that by expanding to the full range examined in the rest of this study with a larger number of experiments, silane concentration would become a significant factor since density which often correlates with thermal conductivity in aerogels[23] is highly influenced by silane concentration. However, even with this limited range of experiments, thermal conductivity was found to significantly increase with increasing water concentration especially when di-isocyanate concentration was also high as shown in a graph of the model in Figure 14. Increasing the number of washes significantly decreases the thermal conductivity.

Although the highest density predicted run did have the highest thermal conductivity of those samples measured, the measured values did not necessarily scale with density. The monolith from run 35, for example, has a density of 0.184 g/cm^3 with thermal conductivity measured at 20 mW/m•K while those produced from run 30 have almost exactly the same density but a thermal conductivity 14 mW/m•K higher. The monoliths from runs 30 and 35 also have very similar-sized cross-links (~19 HDI repeat units) and porosity (86-87%). Scanning electron micrographs of the optimum runs, presented in Figure 15, also appear very similar in appearance. However, the surface areas of the monoliths

produced from run 35 are almost double those from run 30 and the pore sizes are smaller. Hence, a more tortuous path for gas phase conduction in run 35 may decrease k compared to run 30 even though density is similar. It is interesting to note that, similar to thermal conductivity, water and number of washes before cross-linking also have the most dominant effect on surface area (as seen in Figure 7b and 7c), though the trends are the opposite—surface area increases with increasing number of washes and decreases with increasing water concentration.

Conclusions.

Clearly, initial silane, water and di-isocyanate concentration, and the number of washings after gelation and before polymerization have a profound effect on the chemistry and nanostructure of the polymer cross-linked aerogel monoliths produced from a backbone of amine-modified silica cross-linked with di-isocyanates. We have presented mechanistic evidence and quantified the size of the cross-links by utilizing solid ^{13}C NMR and related this insight to other properties of the aerogels. We have also demonstrated that using a balanced amount of silane and water in the initial sol helps to shorten processing by reducing the number of washings necessary to produce a highly porous structure. Even more important is the effect of these processing parameters on properties such as density, porosity, thermal conductivity and strength.

Experimentally, we have generated models for predicting properties of these cross-linked aerogels in a wide range of densities by controlling these four processing parameters. We have demonstrated the utility of these models by applying them to maximize strength and shorten processing time, while preserving low density and high porosity in the final monoliths. We have also verified the prognostic power of the models by producing a series of seven aerogel samples, measuring their properties, and comparing them to predictions for those properties. Thus, cross-linked aerogel monoliths have been demonstrated with comparable compressive strength to those of the previous best at less than half the density, or as much as 130% stronger at two thirds of the density of the previous best. The ultimate

goal is to produce polymer cross-linked aerogels with the desired combination of properties for a particular application.

Supporting Information Available: Appendix I. Table of coefficients from statistical models.

Table 1. Summary of data for di-isocyanate cross-linked monoliths from the experimental design.

Run	Total silane mol/l in solution A	Di-isocyanate w/w %	H_2O mol/l in solution B	No. of washes	Density, g/cm^3	No. of repeat units	Modulus Mpa	Yield 0.2% Strain Mpa	Max. stress at break Mpa	Porosity, (%)	Mean Pore diameter nm	Surf Area m^2/g
1	0.48	33.9	4.30	4	0.071	19.88	0.32	0.019	a	94.6	24	195
2	0.44	33.9	15.27	4	0.124	55.05	2.30	0.097	a	90.2	23	275
3	1.16	20.4	8.93	4	0.191	20.73	8.12	0.245	220.79	85.4	17	245
4	0.48	6.89	4.32	4	0.060	10.79	0.17	0.014	a	96.6	29	207
5	1.16	33.9	8.93	4	0.190	16.87	8.60	0.249	186.90	85.9	18	309
6	2.01	20.4	8.26	4	0.252	12.48	17.48	0.575	139.91	81.7	15	282
7	0.44	6.89	15.27	4	0.114	18.34	1.97	0.087	a	91.8	24	275
8	1.16	20.4	8.93	4	0.198	16.35	8.49	0.284	223.45	85.3	17	289
9	1.22	20.4	4.04	4	0.145	14.53	1.56	0.069	a	89.4	26	194
10	1.91	33.9	13.37	4	0.315	13.58	28.50	1.089	261.26	76.4	15	269
11	1.91	6.89	13.37	4	0.245	9.65	20.29	0.647	170.93	82.1	10	207
12	1.16	20.4	8.93	4	0.181	15.52	4.87	0.179	221.99	86.2	18	252
13	0.46	20.4	9.50	4	0.080	24.59	0.39	0.020	a	93.9	29	252
14	1.10	20.4	14.41	4	0.212	25.53	15.11	0.435	233.34	83.8	18	271
15	2.10	6.89	3.72	4	0.195	6.00	2.47	0.115	78.12	86.0	20	261
16	2.10	33.9	3.72	4	0.243	12.81	5.73	0.232	72.56	82.1	21	232
17	1.16	6.89	8.93	4	0.160	13.10	4.42	0.154	187.86	88.1	19	320
18	1.16	20.4	8.93	4	0.183	14.85	6.73	0.230	203.39	86.4	19	314
19	0.48	6.89	4.32	0	0.081	8.24	0.23	0.018	a	94.4	24	174
20	0.44	6.89	15.27	0	0.342	72.30	48.68	1.796	26.62	72.9	24	94
21	0.48	20.4	4.32	2	0.076	15.45	0.20	0.014	a	94.9	26	202
22	0.48	33.9	4.32	0	0.254	49.29	b	b	b	79.4	24	92
23	0.44	33.9	15.27	0	c	596.75	c	c	c	c	c	8.3
24	1.10	6.89	14.41	2	0.233	16.20	16.87	0.565	184.47	82.5	18	276
25	2.10	6.89	3.72	0	0.371	2.99	29.78	1.070	28.41	73.6	14	248
26	1.91	6.89	13.37	0	0.397	14.19	93.49	2.649	44.10	69.5	12	142
27	2.10	33.9	3.72	0	0.523	3.73	77.29	3.351	39.16	62.8	15	167
28	2.01	33.9	8.26	2	0.357	15.71	64.00	1.699	101.33	73.0	14	227
29	1.91	33.9	13.37	0	c	39.88	c	c	c	c	19	8.6

[a]Monoliths pancaked without true breakpoint; [b]Monoliths shrunk in the middle more than at the ends and were too misshapen to test; [c]Polymer grew outside of gels—monoliths very misshapen.

Table 2. Summary statistics and significant terms for empirically derived models; s = [total silane], d = [di-isocyanate], h = [water], and w = number of washes.

Responses	Significant terms	R^2	Standard (RMS) error
Residual water	$s, h, w, s*w, h*w, h^2$	0.99	313 υg/ml
Density (log transformed)	$s, d, h, w, s^2, w^2, s*d, s*w, s*h$	0.99	0.072 g/cm^3
Porosity	$s, d, w, h, w^2, s*d, d*w, h*w$	0.94	2.16 %
No. of repeats (log transformed)	$s, d, w, h, s^2, s*h, d*h, h*w$	0.94	0.259
Average pore diameter	$s, d, w, h, d^2, h^2, s*d, d*h, h*w, d*w$	0.94	1.403 nm
Surface area (log transformed)	$s, d, w, h, w^2, h^2, s*h, d*h, h*w$	0.91	0.2824 m^2/g
Modulus (log transformed)	$s, d, t, s^2, d*t$	0.97	0.390 MPa
Yield stress (log transformed)	$s, d, w, h, s^2, w^2, s*d, d*w, h*w$	0.98	0.290 MPa
Stress at failure (log transformed)	$s, d, w, h, s^2, w^2, s*d, d*w, h*w$	0. 97	0.162 MPa
Thermal conductivity[a] (log transformed)	$w, h, d*h$	0.99	0.05 mW/m-K

[a]Since only six data points are available, only linear and interactive effects were considered for this model.

24

Table 3. Measurement of residual water after each of four washings for selected number of runs.

Run	Total silane mol/l	H_2O mol/l	Residual water, ug/ml			
			Wash 1	Wash 2	Wash 3	Wash 4
1	0.48	4.30	4305	1030	264	132
2	0.44	15.27	14148	2311	506	248
3	1.16	8.93	7430	2060	436	148
5	1.16	8.93	8338	1940	368	144
6	2.01	8.26	5748	1213	336	132.8
9	1.22	4.04	2786	912	230	128
10	1.91	13.37	9872	2124	468	164
13	0.46	9.50	9818	2278	439	176
14	1.10	14.41	11506	2586	484	142
15	2.10	3.72	254	152	348	70

Table 4. Summary of data for optimized aerogel monoliths.

Run	Total silane (mol/l)	Di-isocyanate (%)	H_2O (mol/l)	Washes	Density, g/cm^3	No. of repeat units	Modulus Mpa	Yield 0.2% Strain (Mpa)	Max. stress at break (Mpa)	Porosity, (%)	Pore size (nm)	Surf Area (m^2/g)	Thermal cond. mW/m-K
30	1.07	13.88	4.11	0	0.181	18.73	4.30	0.238	183.92	87.3	23	142	34
31	0.86	14.6	4.78	1	0.110	15.28	0.51	0.038	a	91.4	28	193	23
32	0.82	19.3	4.20	0	0.136	18.73	1.55	0.086	a	89.8	26	193	25
33	0.44	6.89	4.34	3	0.051	8.55	0.13	0.008	a	93.2	28	163	b
34	1.52	29.7	13.88	4	0.304	24.38	32.20	1.139	237.15	76.9	14	147	36
35	1.27	18.9	7.37	2	0.184	19.16	6.48	0.166	152.06	86.5	20	260	20
36	1.04	6.9	4.12	3	0.119	13.81	0.66	0.050	a	89.5	25	207	19

[a]Monoliths pancaked without a true breakpoint; [b]Sample could not be opacified with gold coating.
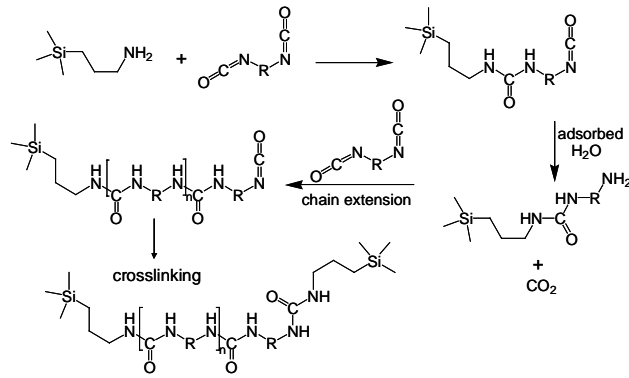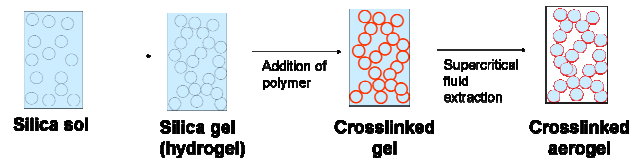
Scheme 1. Mechanism of cross-linking amine modified silica aerogels with di-isocyanate.
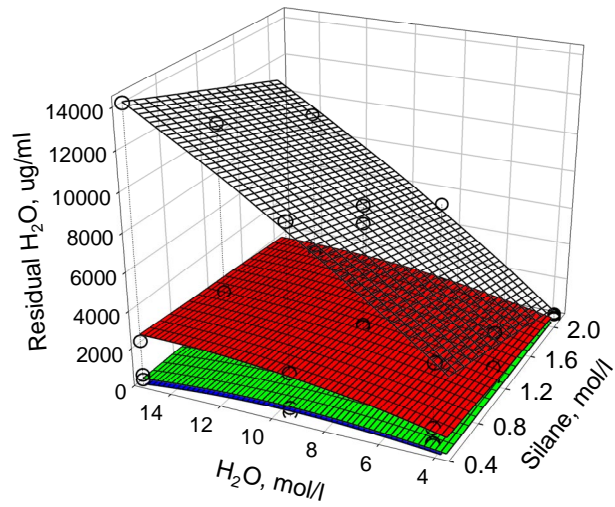
Figure 1. Plot of residual water removed in each wash. (wash 1: clear; wash 2: red; wash 3: green; wash 4: blue.)
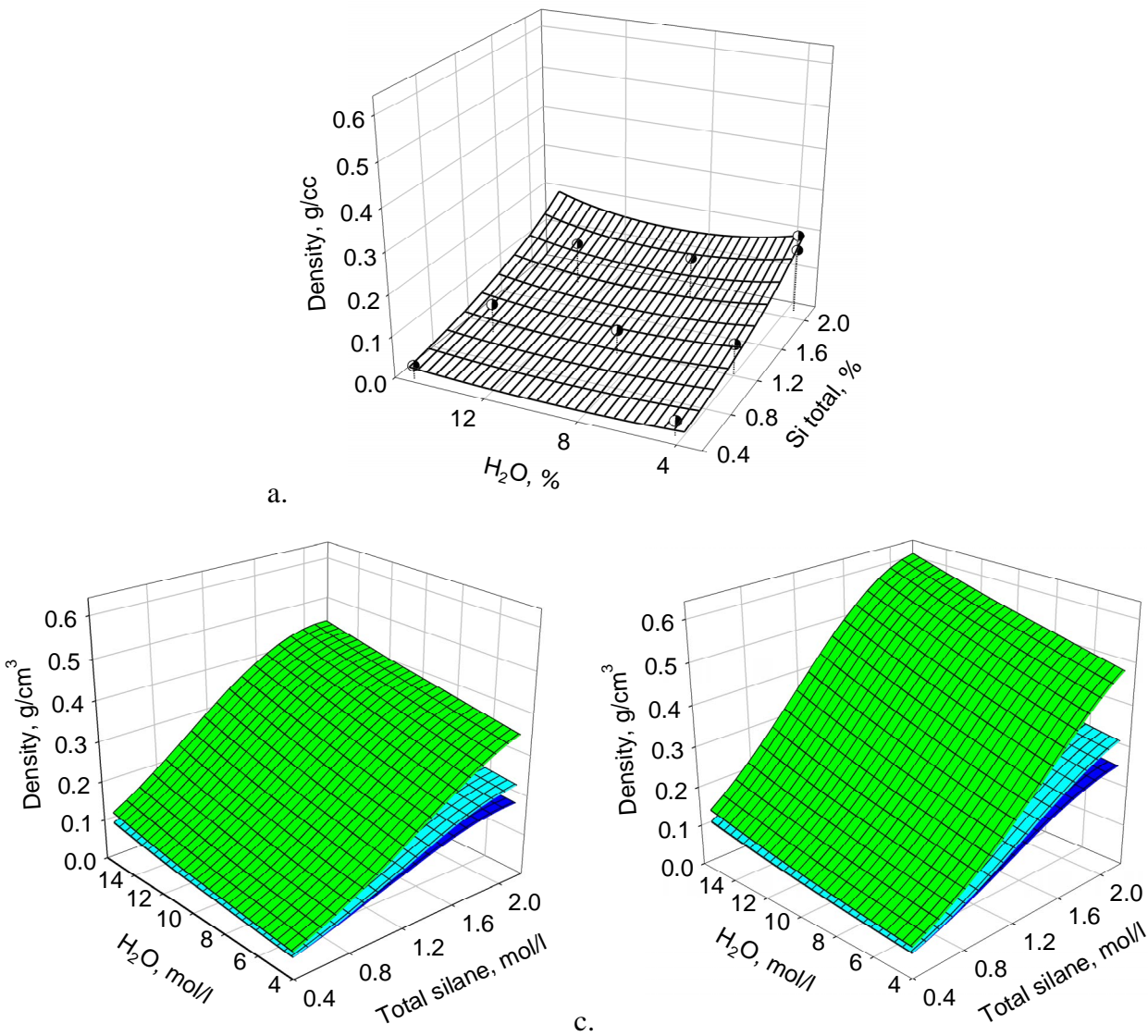
Figure 2. Empirically derived graphs showing density *vs.* total silane and water concentration where a) the samples are not crosslinked; b) di-isocyanate concentration is 6.89 w/w%; and c) 33.9 w/w%. (Green: no washes, cyan: 2 washes, blue: 4 washes.)
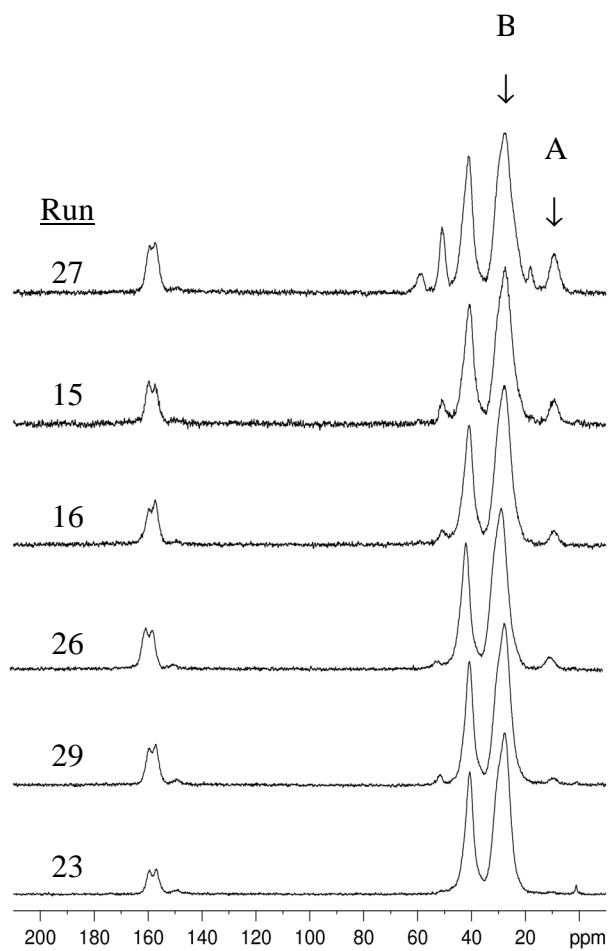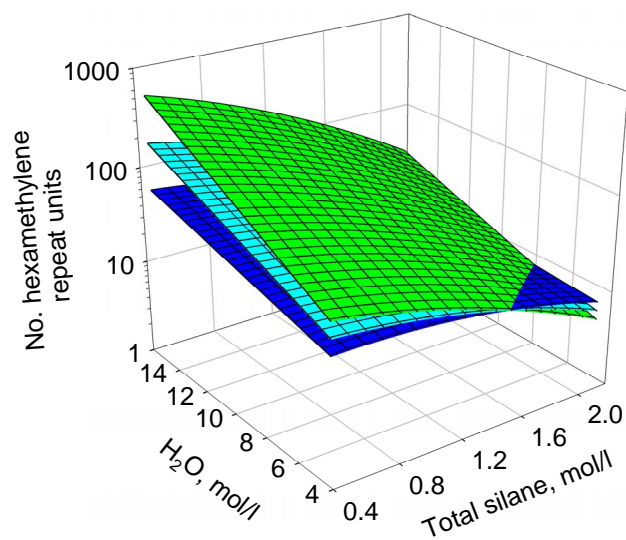
Figure 3. CP-MAS ^{13}C NMR of aerogels cross-linked with increasing chain the length of di-isocyanate cross-link from 3 to 600 repeat units (top to bottom).
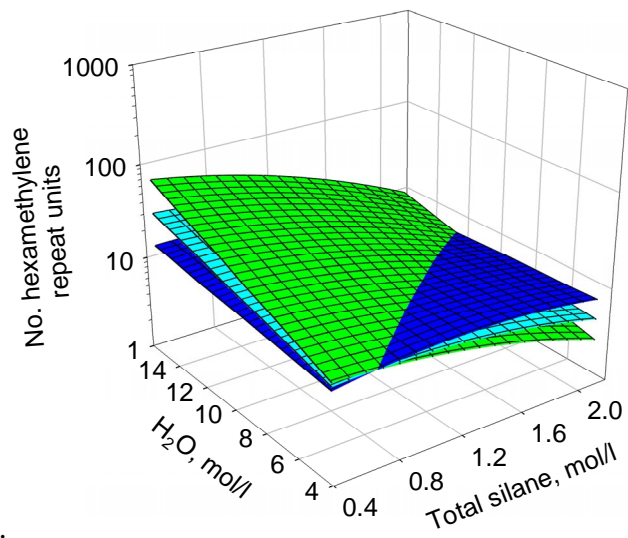
a.

b.

Figure 4. Empirically derived graphs showing number of repeat units as measured by end group analysis *vs*. total silane and water concentration where di-isocyanate concentration is a) 6.89 w/w % and b) 33.9 w/w % . (Green: no washes, cyan: 2 washes, blue: 4 washes.)

a. run 19; d = 0.081g/cm^3 b. run 4; d = 0.060 g/cm^3

c. run 20; d = 0.342g/cm^3 d. run 7; d = 0.114g/cm^3

e. run 23; d = ??? g/cm^3 f. run 2; d = 0.124g/cm^3

g. run 27; d = 0.523 g/cm^3 h. run 16; d = 0.243g/cm^3

i. run 29; d = ??? g/cm^3 j. run 10; d = 0.315 g/cm^3
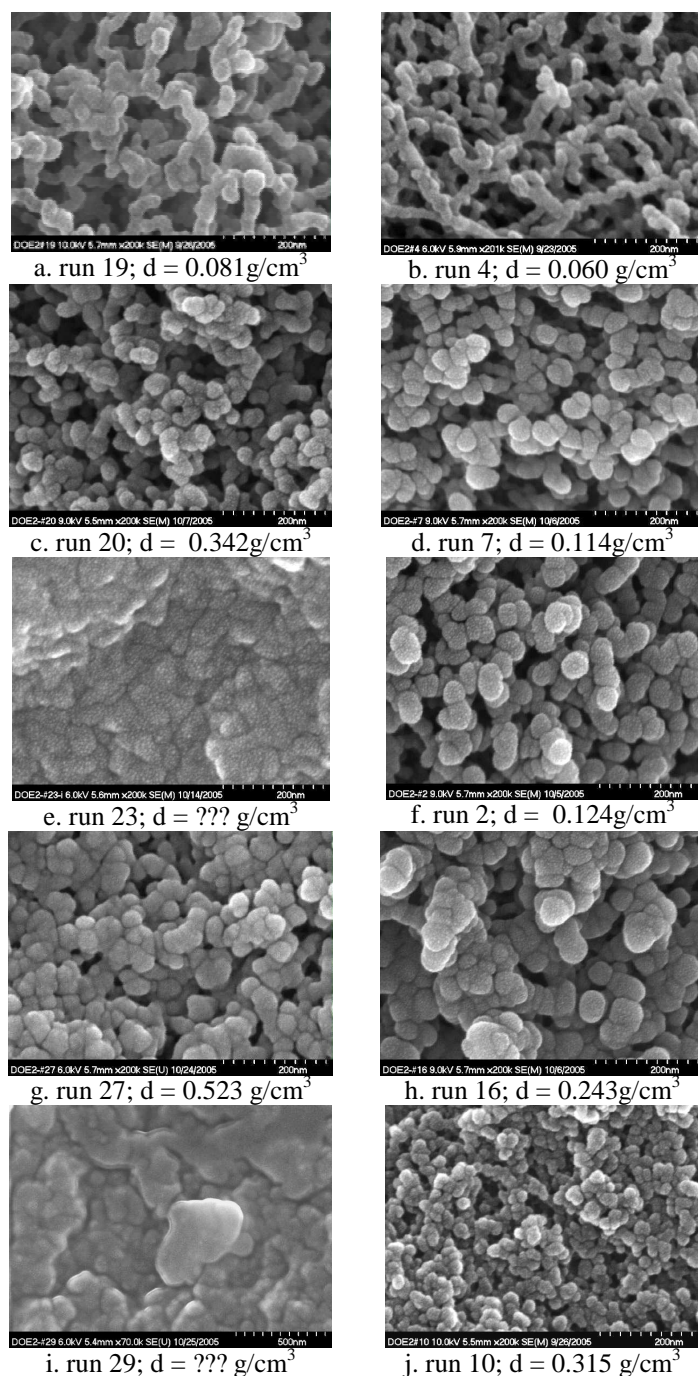
Figure 5. Scanning electron micrographs of monoliths comparing 0 washings on the left and 4 washings on the right for a) and b) low concentrations of silane, water and polymer; c) and d) low concentrations of silane and polymer, high water; e) and f) low concentration of silane, high water and polymer; g) and h) high concentrations of silane and polymer, low water; i) and j) high concentrations of silane, water and polymer.
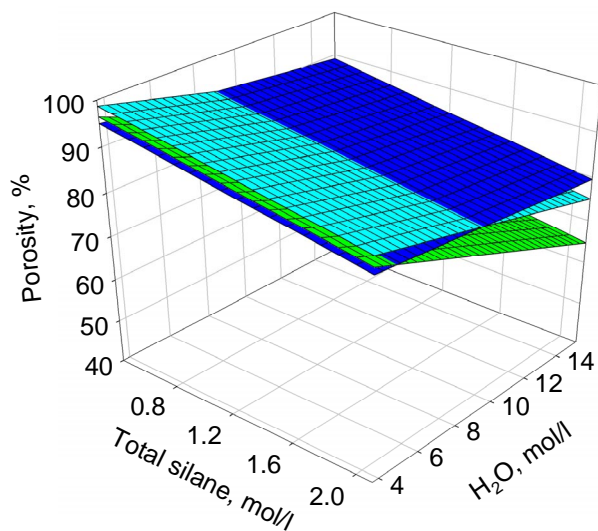
a.
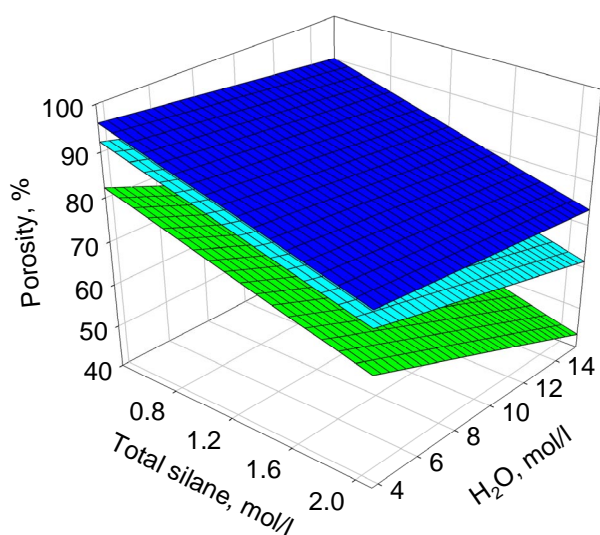
b.

Figure 6. Empirically derived graphs showing porosity *vs*. total silane and water concentration where
a) di-isocyanate concentration is 6.89 w/w % and b) 33.9 w/w %. (Green: no washes, cyan: 2 washes,
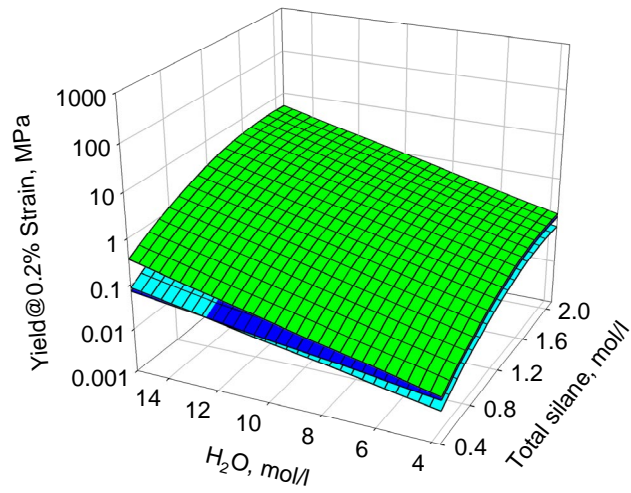blue: 4 washes.)
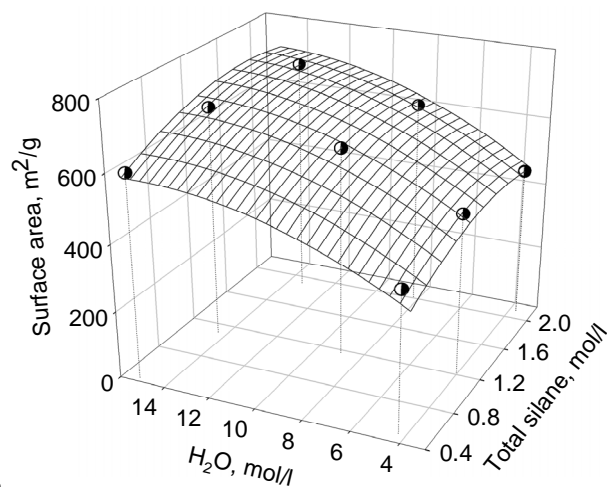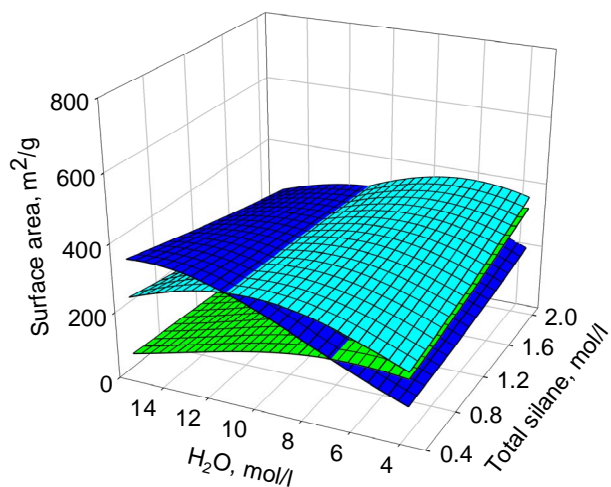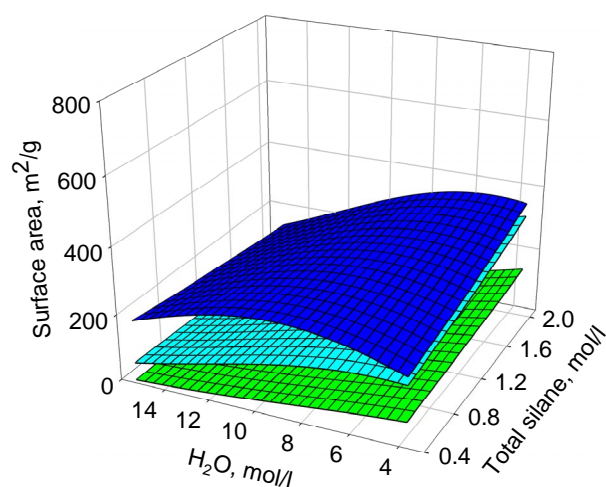
Figure 7. Empirically derived graphs showing surface area as measured by BET analysis *vs.* total silane and water concentration where a) the samples are not cross-linked; b) di-isocyanate concentration is 6.89 w/w % and c) 33.9 w/w %. (Green: no washes, cyan: 2 washes, blue: 4 washes.)
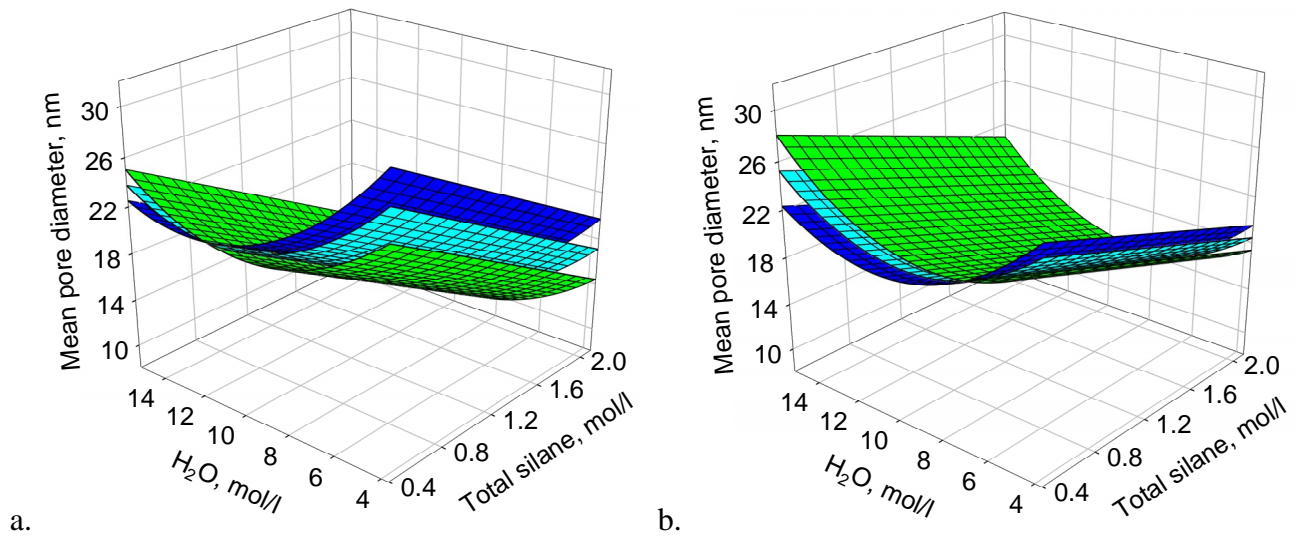
Figure 8. Empirically derived graphs showing mean pore diameter by BET analysis *vs.* total silane and water concentration where a) di-isocyanate concentration is 6.89 w/w % and b) 33.9 w/w %. (Green: no washes, cyan: 2 washes, blue: 4 washes.)
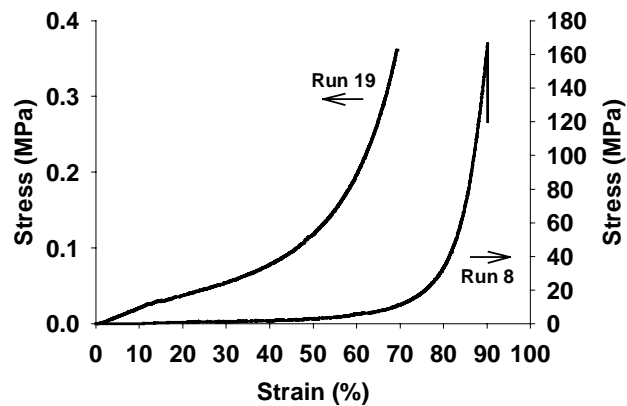
Figure 9. Stress-strain curves for selected runs showing range of strengths from different density samples. Arrows indicate correct axis for each plot.
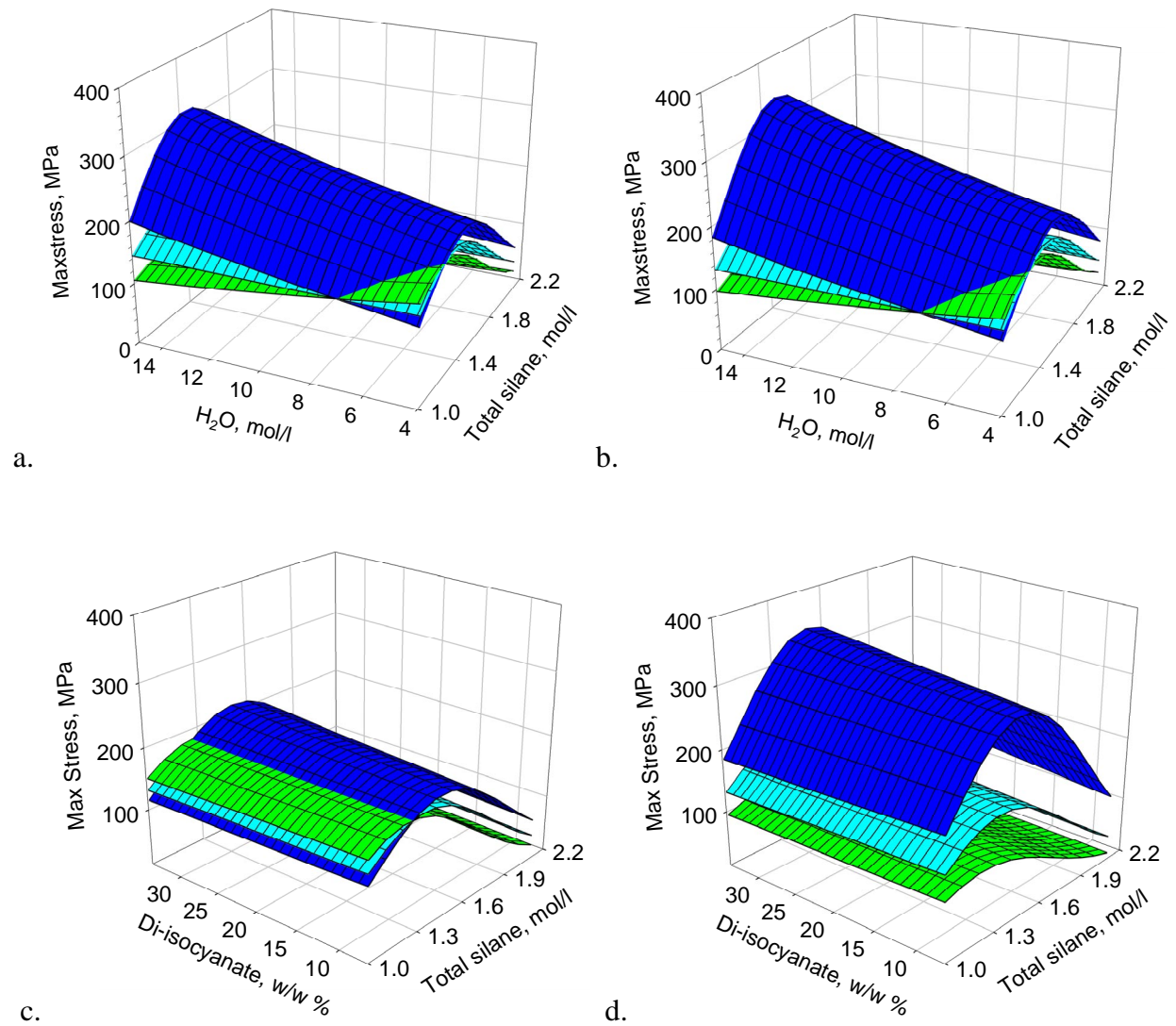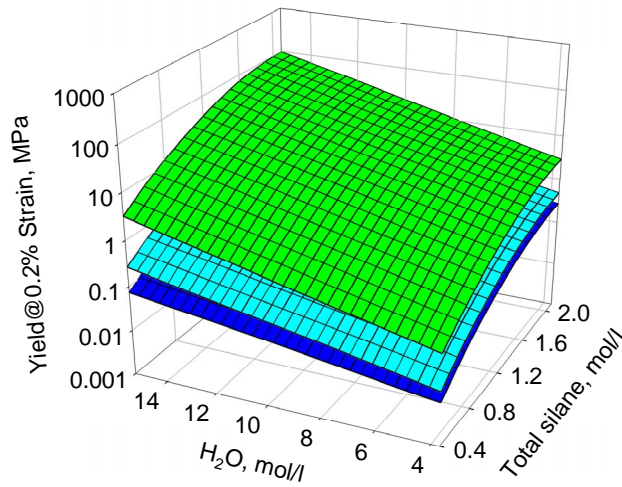
Figure 10. Empirically derived graphs showing maximum stress at break *vs*. total silane and water concentration where a) di-isocyanate concentration is 6.89 w/w % and b) di-isocyanate concentration is 33/9 w/w %; and maximum stress at break *vs*. total silane and di-isocyanate concentration where c) water concentration is 3.7 mol/l; and d) water concentration is 15.3 mol/l. (Green: no washes, cyan: 2 washes, blue: 4 washes.)
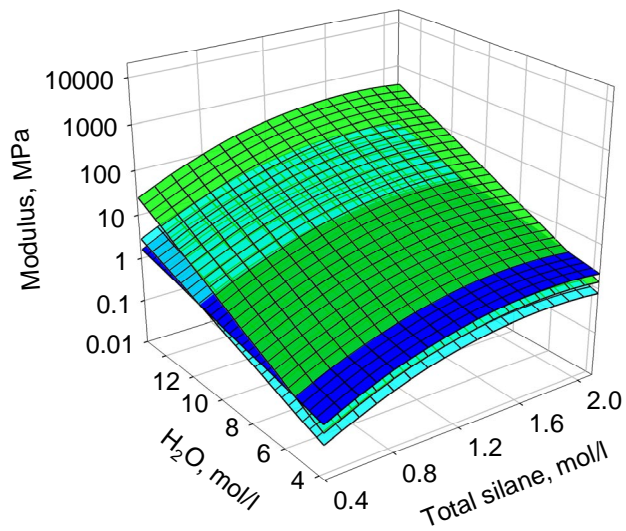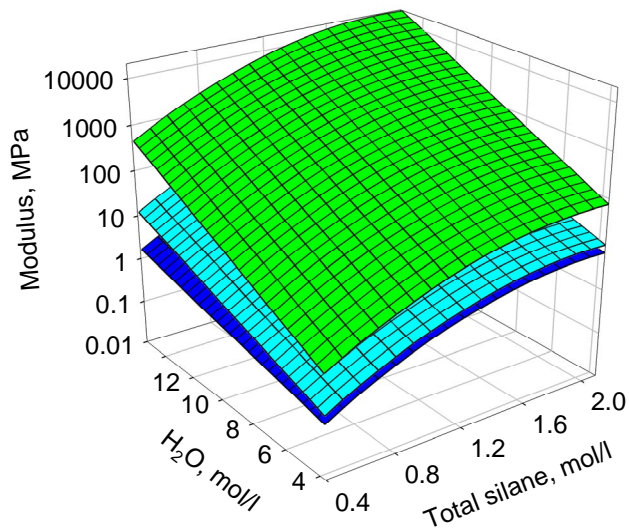
Figure 11. Empirically derived graphs showing yield at 0.2% strain *vs*. total silane and water concentration where a) di-isocyanate concentration is 6.89 w/w %; b) 33.9 w/w %. (Green: no washes, cyan: 2 washes, blue: 4 washes.)

a.

b.

Figure 12. Empirically derived graphs showing modulus *vs*. total silane and water concentration where
a) di-isocyanate is 6.89 w/w %; b) 33.9 w/w %. (Green: no washes, cyan: 2 washes, blue: 4 washes.)
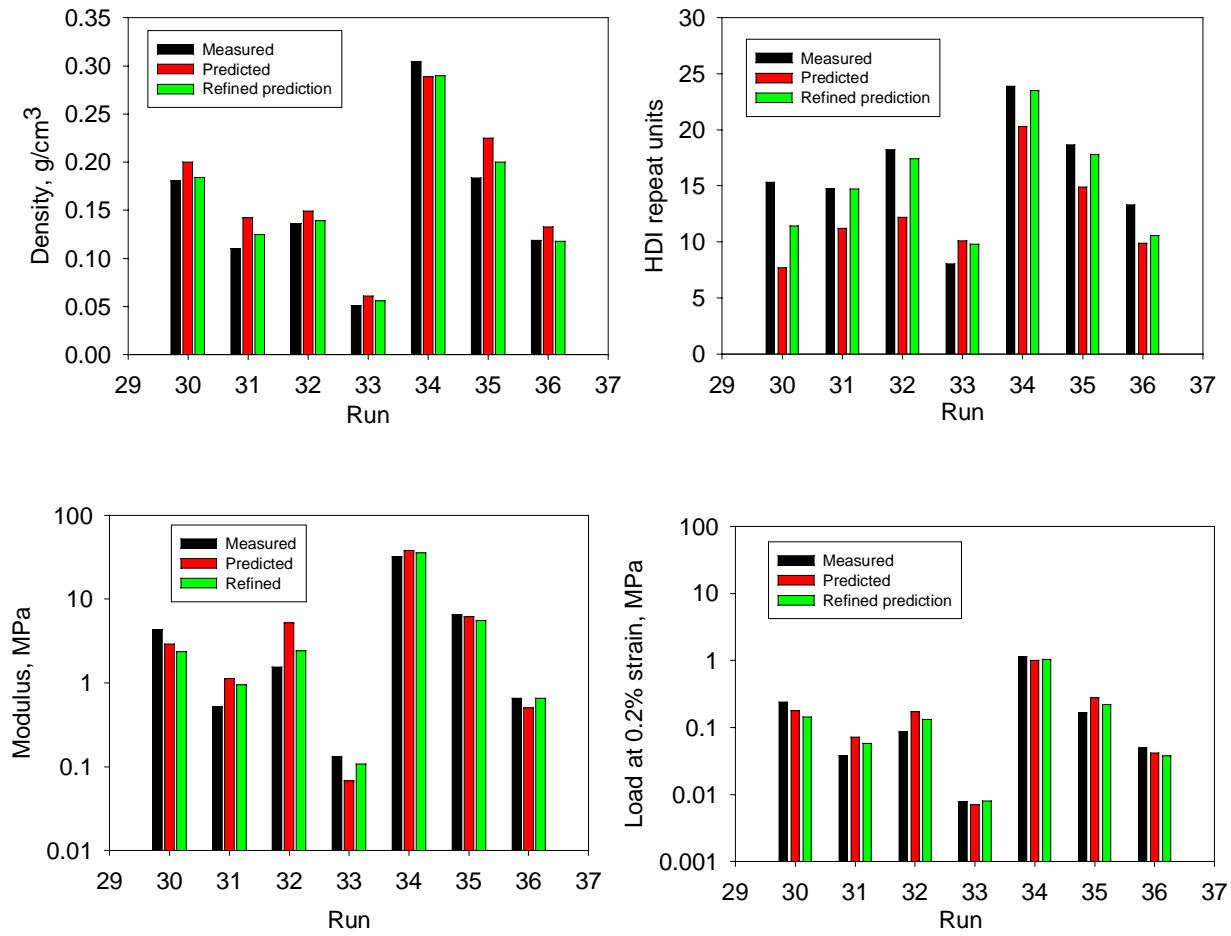
Figure 13. Select data from optimum runs compared to that predicted from the models.
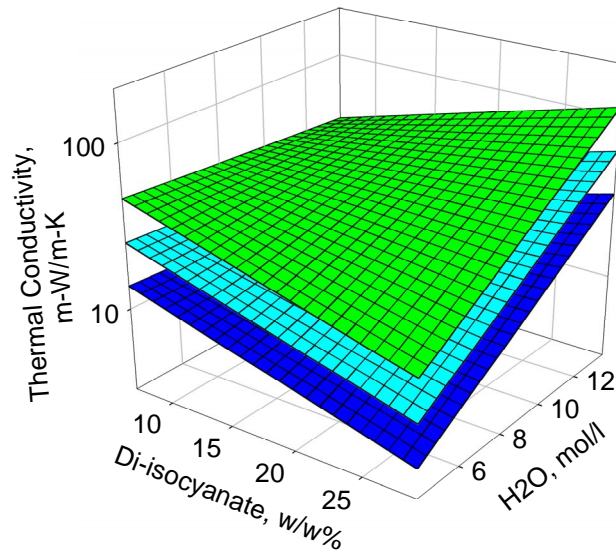
Figure 14. Empirically derived graphs showing screening model of thermal conductivity *vs.* di-isocyanate and water concentration. (Green: no washes, cyan: 2 washes, blue: 4 washes.)

a. run 30; d = 0.181 g/cm^3;
k = 34 mW/m-K
Surface area = 142 m^2/g

b. run 35; d = 0.184 g/cm^3;
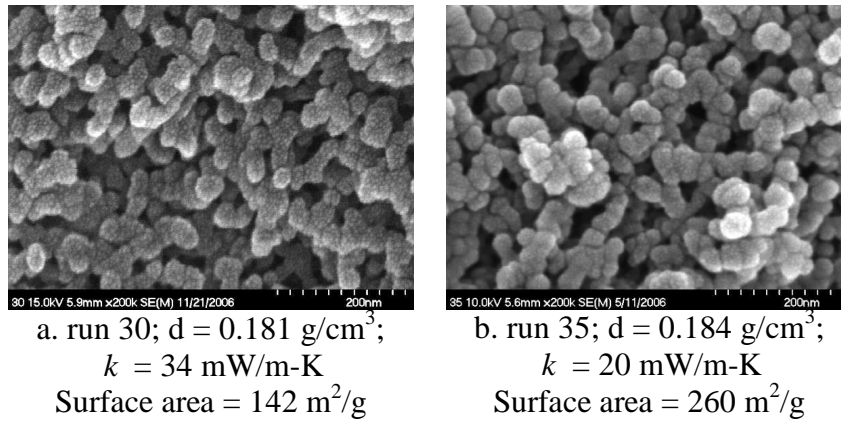k = 20 mW/m-K
Surface area = 260 m^2/g

Figure 15. Scanning electron micrographs of selected optimum aerogel monoliths with similar

densities but different surface areas and thermal conductivity values.

References

(1)   Pierre, A. C., Pajonk, G. M., *Chem. Rev*. **2002**, 102, 4243-4265; Morris, C. A.; Anderson, M. L.; Stroud, R. M.; Merzbacher, C. I.; Rolison, D. R., *Science* **1999**, *284*, 622-624; Pajonk, G. M., *Catal. Today* **1999**, *52*, 3-13; Fricke, J.; Arduini-Schuster, M. C.; Buttner, D.; Ebert, H.; Heinemann, U.; Hetfleisch, J.; Hummer, E.; Kuhn, J.; Lu, X., In *Thermal Conductivity 21*, Cremers, C. J.; Fine, H. A., Eds. Plenum Press: New York, 1990; pp 235-245.

(2) Jones, S. M, *Journal of Sol-Gel Science and Technology*, **2006**, *40*, 351-357.

(3) Novak, B. M.; Auerbach, D.; Verrier, C., *Chem. Mater*. **1994**, *6*, 282-286

(4) Kramer, S. J.; Rubio-Alonso, F.; Mackenzie, J. D., *Mater. Res. Soc. Symp. Proc*, **1996**, *435*, 295-300.

(5) Premachandra, J. K.; Kumudinie, C.; Mark, J. E.; Dang, T. D.; Arnold, F. E., *J. Macromol. Sci., Part A: Pure and Appl. Chem.*, **1999**, *A36*, 73-83.

(6)   Leventis, N.; Sotiriou-Leventis, C.; Zhang, G. H.; Rawashdeh, A. M. M., *Nano Lett.* **2002**, *2*, 957-960.

(7)   Zhang, G. H.; Dass, A.; Rawashdeh, A. M. M.; Thomas, J.; Counsil, J. A.; Sotiriou-Leventis, C.; Fabrizio, E. F.; Ilhan, F.; Vassilaras, P.; Scheiman, D. A.; McCorkle, L.; Palczer, A.; Johnston, J. C.; Meador, M. A.; Leventis, N., *J. Non-cryst. Solids* **2004**, *350*, 152-164.

(8)   Meador, M. A. B.; Fabrizio, E. F.; Ilhan, F.; Dass, A.; Zhang, G. H.; Vassilaras, P.; Johnston, J. C.; Leventis, N., *Chem. Mater.* **2005**, *17*, 1085-1098.

(9) Katti, A.; Shimpi, N.; Roy, S.; Lu, H.; Fabrizio, E. F.; Dass, A.; Capadona, L. A.; Leventis, N. *Chem. Mater*. **2006**, 18, 285-296.

(10) Capadona, L. A.; Meador, M. A. B.; Alunni, A.; Fabrizio, E. F.; Vassilaras, P.; Leventis, N. *Polymer*, **2006**, *47*, 5754-5761.

(11) The complete range of cylindrical dimensions included diameters of 15.5 mm-19.4 mm, representing shrinkage from the 20 mm diameter molded size from 3 to 20%. The large shrinkages are from a few runs (20, 25, 26 and 27) where the samples were not washed before soaking in di-isocyanate. Specimens from these runs could also be described as "loosely cylindrical" being a bit deformed in the middle. More typically, shrinkages ranged from 3 to 7%.

(12) Brinker, C. J.; Scherer, G. W. *Sol-Gel Science*, **1990**, Academic Press, Inc., San Diego, CA 92101.

(13) For more on statistical experimental design, see Montgomery, D. C. *Design and Analysis of Experiments*, 5th Edition, John Wiley and sons, 2001.

(14) Note that the four washes are necessary to supercritically dry the uncross-linked wet gels. Otherwise, water remaining in the gels, especially with no washes, would cause the aerogel structures to collapse.

(15) According to reference 8, based on the stoichiometry for gelation, the theoretical minimum water to TMOS mole ratio, R, needed is 2:1. Since these are mixtures of APTES and TMOS in a 1:3 ratio by volume and APTES has only 3 hydrolyzable alkoxy groups, R in this case is actually closer to 1.8:1.

(16) As discussed in Ref. 9, full elastic recovery for samples with densities of 0.48 g/cm^3 was only experienced in the initial linear elastic region of the stress-strain curve (up to 4% strain). Partial recovery was experienced for up to ~40% strain, while above 60% strain, almost no elastic recovery was evident. Though the initial linear region increases to as much as 10% strain for lower density

samples in this study, examination of recovery through load-unload testing was not carried out. This is a subject for future work.

(17) Smith, D.M.; Maskara, A.; Does, U. *J. Non Crys. Sol.* **1998**, *225*, 254-259.

(18) Parker, W.J.; Jenkins, R.J.; Abbott, G.L. *J. Appl. Phys.* **1961**, *32,* 1679.

(19) Cowan, R.D. *J. Appl. Phys.* **1963**, *34*, 926.

(20) Clark, L.M.; Taylor, R.E. *J. Appl. Phys.* **1975**, *46*, 714.

(21) Lee, D.; Stevens, P.C.; Zeng, S.Q.; Hunt, A.J. *J. Non Crys Sol*. **1995**, *186*, 285-290.

(22) Rettelbach, T.; Säuberlich, J.; Korder, S.; Fricke, J. *J. Non. Crys. Sol.* **1995**, *186*, 278-284.

(23) Husing, N.; Schubert, U. *Angew. Chem. Int. Ed*. **1998**, *37*, 22-45.